Modeling the influence of temperature and water potential on seed germination of *Allium tenuissimum* L.

Hong Xiao[1], Helong Yang[1], Thomas Monaco[2], Qian Song[1], Yuping Rong[1]

[1] Beijing Key Laboratory of Grassland Science, College of Grassland Science and Technology, China Agricultural University, Beijing 100193, China

[2] USDA-ARS Forage and Range Research Laboratory, Utah State University, Logan, UT 84322-6300, USA.

Corresponding author:
Yuping Rong[1]
Beijing Key Laboratory of Grassland Science, College of Grassland Science and Technology, China Agricultural University, Beijing 100193, China.
Email address: rongyuping@cau.edu.cn

Abstract

Allium tenuissimum L. is a widely distributed perennial herbaceous species in temperate and desert steppes. Relative to other wild *Allium* species, it produces unique sweet flavors, more biomass in arid and cold environments, and has generated greater interest for crop production. Successful crop establishment, however, will depend on rapid and uniform seed germination. Our study aimed to characterize seed germination of *A. tenuissimum* under various temperature regimes (11, 15, 20, 24 and 28 °C) and water potential levels (0, -0.2, -0.4 and -0.6 MPa), and model germination by hydrotime (HT) and hydrothermal time (HTT) analysis. Final germination percentage (FGP) increased within the range of 11 to 20 °C, yet it declined within the range of 24 to 28 °C and generally decreased as water potential became more negative within each temperature setting. Maximum FGP was observed at 20 °C at all water potential settings and ranged from 55.0 ± 5.3 to 94.8 ± 1.4 %. According to HT and HTT models, the base (T_b) and optimum temperatures (T_o) for seed germination were 7.0 and 20.5 °C, respectively. In addition, base water potential for the fraction of germination within the seed lot ($\Psi_b(g)$) shifted to 0 MPa as temperature increased from T_b to ceiling temperature (T_c). For obtaining 50 % seed germination, $\Psi_b(50)$ and $T_c(50)$ were estimated to be -0.67 MPa and 27.2 °C, respectively. These values for T_b and $\Psi_b(50)$ suggest seed germination of *A. tenuissimum* is both cold and drought tolerant and suitable for production in semi-arid regions. Our characterization of the ideal sowing conditions for *A. tenuissimum*, i.e., 20.5 °C and soil water potential less negative than -0.67 MPa offers information to forecast suitable settings to enhance crop production.

Introduction

Seed germination is an essential process in establishing stable plant populations and is regulated by many environmental factors (*Atashi et al., 2015*; *Juan-Vicedo et al., 2016*). Among these factors, temperature and moisture conditions strongly regulate germination dynamics (*Bakhshandeh and Gholamhossieni, 2019*), and characterizing the base, optimum, and ceiling temperatures is one way of describing how temperature influences seed germination dynamics (*Bakhshandeh et al., 2013*; *Bewley et al., 2013*). Furthermore, thermal time (TT) models can be applied to predict seed germination dynamics across a range of temperatures (*Mccartan et al., 2015*; *Bidgolya et al., 2018*; *Trudgill et al., 2005*) and have proven useful in estimating germination under the dynamic temperatures of field seedbeds (*Rawlins et al., 2012*; *Izquierdo et al., 2013*). However, TT models may inaccurately predict seed germination responses under supra-optimal temperature ranges (*Bakhshandeh et al., 2015*; *Bradford, 2002*).

Germination is also very sensitive to moisture conditions and water deficiency-induced osmotic stress is known to prevent seed germination or slow germination rates (*Tobe et al., 2001*). Accordingly, water status is typically reported as osmotic water potential, and hydrotime (HT) models are typically applied to simultaneously account for changes in both final germination percentage and germination rate across variable water potential levels (*Soltani et al., 2017*; *Bakhshandeh and Gholamhossieni, 2018*). Furthermore, the combination of HT and TT models have produced hydrothermal time (HTT) models (*Alvarado and Bradford, 2002*;

58 *Gummerson, 1986*) capable of determining the hydrothermal accumulation for seed germination
59 at various temperature and water potential conditions and predict the time course of seed
60 germination even across sub-optimal (*Gummerson, 1986*) and supra-optimal temperature ranges
61 (*Alvarado and Bradford, 2002*). Consequently, parameters of HTT models can be used to
62 characterize the physiological status of seed populations in response to variable temperature and
63 water potential and have been widely applied to predict germination dynamics in numerous crops
64 such as safflower (*Carthamus tinctorius*) (*Bidgolya et al., 2018*; *Torabi et al., 2016*), sesame
65 (*Sesamum indicum*) (*Bakhshandeh et al., 2017*), zucchini (*Cucurbita pepo*) (*Atashi et al., 2015*),
66 and watermelon (*Citrullus vulgaris* cv. 'Crimson sweet') (*Bakhshandeh et al., 2015*) and other
67 wild species (*Abdellaoui et al., 2019*; *Fakhfakh et al., 2018*; *Horn et al., 2015*).
68   *Allium tenuissimum* L. is a perennial herbaceous species distributed in temperate and desert
69 steppes of north-central Asia (*He, 2008*; *Li et al., 2011*). Within these ecosystems, it plays a
70 critical role in sand fixation and conservation of water and soil due to having a well-developed
71 fibrous root system and high tolerance of environmental stresses (*Zhao, 2010*). It is also
72 recognized as a high-quality forage for herbivores (*Song et al., 2016*) and has economic
73 importance due to its distinctive and tasty flavor (*Li and Zhang 2011*; *Zhang and Liu, 2012*).
74 Consequently, it is highly valued as a vegetable or food seasoning (*Li and Zhang 2011*; *Liu et al.,*
75 *2016*) and has generated interest in exploring new harvesting methods (Zhang et al., 2014),
76 potential ways to extract essential oil from its flowers (*Zhang and Liu, 2012*), and identifying the
77 unique volatile flavor compounds in flowers of *A. tenuissimum* (*Xu et al., 2017*). Despite these
78 favorable qualities, establishing crops of *A. tenuissimum* on large-scales is not feasible by
79 propagation of bulb tillers, but may become economically viable through propagation by seeds
80 (*Li et al., 2013*; *Zhao et al., 2011*). Therefore, exploring seed germination dynamics under
81 variable environmental conditions is an important step toward industrialized production. In this
82 study, we aimed to focus on the response of seed germination to various temperatures and water
83 potential conditions in *A. tenuissimum*: (i) characterizing seed germination dynamics of *A.*
84 *tenuissimum* using HT and HTT models, and (ii) defining cardinal temperatures and base water
85 potentials for *A. tenuissimum* seeds based on model parameters.

Materials & methods

86

Seed germination

87

88 Seeds of *A. teniussimum* were collected from a temperate desert steppe area in Dongsu County
89 [43°51′36″ N, 113°40′02″ E, 1060 m a.s.l. (meters above sea level)], Inner Mongolia during
90 October 2015 (approved by Yuping Rong, China Agricultural University). After that, the seeds
91 were naturally dried, surface cleaned and put into a sealed glass container, and then stored at 4
92 °C in a refrigerator until needed for experimentation (April 2016).
93   Germination assays were conducted in a growth chamber (SPX-250-GB, Hengyu, China)
94 located at the Grassland Science Department, China Agricultural University, Beijing, China with
95 an 8 h light/16 h dark day/night lighting pattern. The light intensity and relative humidity were
96 set as 6000 lx and 50%. Mature Seeds were sterilized for 5 min with 10 % NaClO and then
97 washed with distilled water (*Rong et al., 2015*). For the germination tests, 100 seeds were placed

98   in glass Petri dishes (90 mm inner diameter) containing two layers of filter paper (1001-090,

99   Whatman, UK) saturated with distilled water ($\Psi = 0$ MPa) or solutions of different water

100   potential levels ($\Psi = -0.2$, -0.4 and -0.6 MPa). Petri dishes were then transferred to the chamber

101   and germination was characterized at four constant temperature settings (11, 15, 20, 24 and 28

102   °C), each replicated four times for each water potential level. Different water potential levels

103   were produced by mixing aqueous solutions of polyethylene glycol (PEG) 6000 with distilled

104   water according to Michel and Kaufmann (1973). A vapour pressure osmometer (Model 5100C,

105   Wescor, Inc., Logan, UT, USA) was used to measure Ψ of solutions and create desired levels for

106   all temperature settings. To maintain constant Ψ and avoid fungal attack, seeds incubated on

107   PEG 6000 solutions were transferred to fresh solutions every 2 d. Germination was scored daily

108   by observing radicle protrusion. Seed germination was defined depend on the length of radicle.

109   Normally seeds were regarded as germinated when the length of radicle was more than 2 mm

110   (*Saleem et al., 2019*). To avoid errors in recording germination, germinated seeds were removed

111   after being counted. Furthermore, germination tests were terminated when no new germinated

112   seeds were counted for three consecutive days.

113 Germination analysis

114   Germination rates (GR_g) were calculated using the equation: $GR_g = 1/t_g$, where t_g is the duration

115   to radicle emergence. Estimations of germination rate for the 50th percentile (GR_{50}) in each

116   replicate were calculated by interpolation using curves fit to the time course data. To determine

117   the optimal germination temperature, germination rates at 20 and 24 °C were compared. If final

118   germination percentage at 20 °C was significantly greater than germination at 24 °C, the optimal

119   temperature was assumed to be 20 °C.

120 HT model

121   The relationship between GR_g and Ψ was described by using the following equation:

122    $$\theta_H = \left[\Psi - \Psi_b(g)\right]t_g \qquad (1)$$

123   where θ_H is the hydrotime (MPa d) constant of the seeds required for germination, $\Psi_b(g)$ is the

124   theoretical threshold or base Ψ that will prevent the germination of fraction g. The parameters in

125   the HT model were estimated according to the equation:

126    $$\text{Probit(g)} = \left[\left(\Psi - \theta_H/t_g\right) - \Psi_b(50)\right]/\sigma_{\Psi b} \qquad (2)$$

127   where $\Psi_b(50)$ is the base water potential for attain the 50th percentile of germination, and $\sigma_{\Psi b}$ is

128   the standard deviation of $\Psi_b(g)$ in seed lots. To examine whether parameters of this model can be

129   accurately used to quantify the sensitivity of seed populations to the variation of Ψ, the [1-

130    $(\Psi/\Psi(g))]t_g$ factor derived from Bradford (1990) was applied to normalize germination time

131   courses at reduced Ψ in this study. Germination time course can be normalized by this factor at

132   any Ψ to the corresponding time course that would occur in water for the seed population using

133   the parameters from the HT model. All normalized data from different temperature conditions

134   were plotted on a common thermal time scale, using the estimated T_b at 0 MPa.

135 HTT model

136   The HTT model describes seed germination patterns when T and Ψ both vary; *Alvarado and*

137 *Bradford, 2002*). The relationship between GR_g and variable conditions of T and Ψ are described
138 by Eq. 3 for sub-optimal T, and modified Eq. 4 for supra-optimal T:

139 $\theta_{HT} = (T - T_b)[\Psi - \Psi_b(g)]t_g$ (3)

140 $\theta_{HT} = \{\Psi - \Psi_b(g) - [K_T(T - T_o)]\}(T - T_b)t_g$ (4)

141 where θ_{HT} is the hydrothermal constant and T_b is the base temperature. In Eq. 4, $[K_T(T - T_o)]$
142 applies only in the supra-optimal range of T and K_T is the slope of the relationship between
143 $\Psi_b(50)$ and temperatures when $T > T_o$; T_o is the optimum temperature. The value of $\Psi_b(g)$ is set
144 equal to the distribution of $\Psi_b(g)$ at T_o, and $(T - T_b)$ is equal to $(T_o - T_b)$. Parameter values in
145 above models can be obtained by probit analysis according to Eq. 5 and Eq. 6 for sub- and supra-
146 optimal T, respectively.

147 $\text{Probit}(g) = [(\Psi - \theta_{HT}/(T - T_b)t_g) - \Psi_b(50)]/\sigma_{\Psi_b}$ (5)

148 $\text{Probit}(g) = [(\Psi - \theta_{HT}/(T - T_b)t_g) - K_T(T - T_o) - \Psi_b(50)]/\sigma_{\Psi_b}$ (6)

149 As described in Alvarado and Bradford (2002), the values of K_T and T_o were varied for
150 germination time courses at $T > T_o$ until a fit was obtained that resulted in values of θ_{HT}, $\Psi_b(50)$
151 and σ_{Ψ_b} matching those obtained at or below T_o.

Statistical analyses

153 A two-way analysis of variance (ANOVA) was carried out using SPSS 19.0 for Windows (SPSS
154 Inc., Chicago, IL, USA) to evaluate the influence of T, Ψ, and their interactions on seed
155 germination variables of *A. teniussimum*. The results showed with mean and SE value of four
156 replicates. All probit analyses of HT and HTT models were fitted in SAS 8.2 statistical package
157 (SAS Institute, Cary, NC, USA) using the PROC PROBIT routine, which employs a maximum-
158 likelihood weighted regression method (*Bradford, 1990*; *Dahal and Bradford, 1994*).

Results

Seed germination in response to temperature and water potential

161 Results of analysis of variance indicated that the final germination percentage (FGP) of *A.*
162 *tenuissimum* seeds was significantly influenced by T ($F=587.9$, $P < 0.0001$), Ψ ($F=643.0$, $P <$
163 0.0001), and their interactions ($F=24.2$, $P < 0.0001$) (Fig. 1, Table S1). When values of Ψ
164 remained constant, FGP increased as T increased within sub-optimal ranges (11 to 20 °C), while
165 it declined within supra-optimal ranges (24 to 28 °C). In distilled water (i.e., $\Psi = 0$ MPa), FGP
166 changed from 72.0 ± 1.4 to 94.8 ± 1.4 % over various T conditions. Maximum FGP was
167 observed at 20 °C under all levels of Ψ and ranged from 55.0 ± 5.3 to 94.8 ± 1.4 %. For all T
168 settings, FGP decreased with decreasing Ψ levels. Few seeds germinated under the combination
169 of -0.6 MPa and 11 °C. In contrast, FGP reached 94.8 ± 1.4 % when seeds were incubated in
170 water at 20 °C, indicating that the seeds in this analysis were non-dormant.

Hydrotime analysis

172 Parameters generated by the HT model are presented in Table 1. Values of θ_H decreased from 6.4
173 MPa d at 11 °C to 4.4, 4.2, 3.0 and 3.0 MPa d at 15, 20, 24 and 28 °C, respectively. This
174 suggests that the time required for germination declined as T increased within sub-optimal

175 ranges, while it remained constant at supra-optimal ranges. Values of $\Psi_b(50)$ increased as T
176 increased from 11 to 28 °C. Notably, estimated values of $\Psi_b(50)$ increased more positively at
177 supra-optimal temperatures, rising from -0.40 MPa at 24 °C to -0.16 MPa at 28 °C. Values of σ_{Ψ_b}
178 varied from 0.20 to 0.37 MPa across all regimes of T. Specifically, values of σ_{Ψ_b} were nearly
179 constant within the range of 15 to 24 °C, indicating that the variation in Ψ_b among all seeds in
180 this *A. tenuissimum* population was small.
181   The curves in Fig. 2a-e are germination time courses predicted by HT model based on the
182 $\Psi_b(g)$ threshold distributions (Fig. 2F-G) and the estimated parameters (Table 1). At each T
183 setting, the predicted curves closely matched actual seed germination data under the various Ψ
184 levels (Fig. 2A-E). Normalization of germination time courses across various Ψ levels at sub-
185 and supra-optimal T levels incorporated into a common curve are shown in Fig. 3. At sub-
186 optimal T, the difference between groupings of normalized observations and common curve is
187 indistinct (Fig. 3A). However, the grouping of normalized observations at 28 °C did not
188 resemble the profile from the common curve and fell into a distinct group (Fig. 3B). This
189 indicates that the estimates of HT model interacted with T. Furthermore, these HT estimates
190 consistently showed the largest shift in Ψ_b with increasing T (Fig. 2F-G) and the grouping of
191 normalized observations accurately predicted seed germination in this population.

Hydrothermal time analysis

193 Parameters for the HTT model, estimated in the sub- and supra-optimal T ranges, are shown in
194 Table 2. The hydrothermal time requirement (θ_{HT}) for seed germination was 43.9 MPa °C d.
195 Values T_b and $\Psi_b(50)$ were estimated to be 7.0 °C and -0.67 MPa, respectively. FGP increased
196 until 20.5 °C (T_o), then it declined towards ceiling temperatures ($T_c(g)$), at which germination
197 theoretically ceased when T exceeded T_o. In addition, $T_c(50)$, the ceiling temperature for
198 germination of 50 %, was 27.2 °C. The estimates for K_T was 0.1 MPa °C^{-1}, indicating that Ψ
199 declined by 0.1 MPa for every degree that T exceeds T_o. Applying the HTT models using the *A.*
200 *tenuissimum* germination data resulted in high R^2 values at both sub-optimal ($R^2 = 0.89$) and
201 supra-optimal ($R^2 = 0.81$) T ranges, indicating a high degree of congruency between predicted
202 and observed germination responses.

Discussion

**Seed germination of *A. tenuissimum* in response to various temperature and
water availability conditions**

206 Successful establishment of cultivated plants depends on rapid and uniform seed germination
207 (*Fakhfakh et al., 2018*; *Bidgolya et al., 2018*); however, suitable water availability and
208 temperature conditions for seed germination are only available during a short period in most arid
209 and semi-arid regions (*Fakhfakh et al., 2018*; *Belo et al., 2014*; *Watt and Bloomberg, 2012*).
210 Here, we presented a comprehensive study of seed germination responses to different
211 temperatures and water potential levels in *A. tenuissimum*, an important wild onion species from
212 temperate-desert steppes of north central Asia (*He, 2008*; *Li et al., 2011*). Our results showed
213 that final germination percentage of *A. tenuissimum* strongly depended on the interaction of these

214   two factors. Furthermore, applying HTT models to our dataset provided insights into suitable
215   conditions to enhance consistent germination responses of this valuable native species. Later, we
216   discuss in detail the nuances of our results that underpin this methodological approach and
217   expedite industrialization of wild species under stressful environmental conditions.
218   Numerous studies have illustrated how temperature-dependent seed germination is related to
219   the geographical and ecological distribution of a particular species such as common vetch (*Vicia*
220   *sativa*) (*Liu, 2010*), *Stipa* species (*Ronnenberg et al., 2008*) and temperate sedges (*Carex*)
221   (*Schütz and Rave, 1999*). For *A. tenuissimum*, the final germination percentage was quite high
222   (i.e., 92.5 to 94.8 %) in the temperature range of 15 to 20 °C (Fig. 1). In some mediterranean
223   grassland species, 15 °C and 20 °C also were found to be the best temperature for seed
224   germination (*Herranz et al., 1998;* Marques and Draper, 2012). In contrast, the lower
225   temperatures for preferable germination of *A. tenuissimum* seeds was consistent with a prior
226   study of wild species of *Allium* distributed in temperate desert steppe (*Zhao et al., 2011*). In any
227   constant temperatures, final germination percentage declined when seeds were incubated at
228   reduced water potential levels (Fig. 1). This response is likely associated with enzyme activity
229   and oxygen availability of seeds, which are known to decrease when germinated at unfavorable
230   temperatures and limiting moisture conditions (*Bewley and Black, 1994*). Furthermore, higher
231   incubation temperatures and more negative values of water potential during germination likely
232   induced secondary dormancy of seeds, leading to prolonged seed germination over non-optimal
233   temperatures and more negative water potential levels (Fig. 2).

234   **Predicting seed germination with mathematical models**
235   Mathematical models to predict and quantify the influence of environmental factors on seed
236   germination are essential when little information is known about the ideal conditions for
237   potential agronomic species such as zucchini (*Cucurbita pepo*) (*Atashi et al., 2015*), red brome
238   (*Bromus rubens*) and cheatgrass (*Bromus tectorum*) (*Horn et al., 2015*), and safflowers
239   (*Carthamus tinctorius*)(*Bidgolya et al., 2018*). While accounting for the influence of only
240   temperature, TT models can successfully predict germination time courses in sub-optimal
241   temperature ranges, but they become less effective at predicting germination in supra-optimal
242   temperature ranges (*Bradford, 2002*; *Bewley et al., 2013*), which spurred the development of
243   hydrothermal models combine the influences of temperature and water availability on seed
244   germination (*Windauer et al., 2012*). Such HT and HTT models have been widely applied and
245   accurately describe seed germination across variable temperatures and water potential levels
246   (*Alvarado and Bradford, 2002*; *Bakhshandeh et al., 2015, 2017*). In addition, normalizing
247   thermal time scales, as we did for the germination time courses of *A. tenuissimum* (*Bradford,*
248   *1990, 2002*), accurately described the influences of temperature and water availability (Fig. 3A).
249   However, the grouping of normalized observations at 28 °C fell into a distinct group instead of
250   resembling the profile from the common curve (Fig. 3B). Similarly, previous studies documented
251   that HT analysis was unable to predict the germination time courses at supra-optimal
252   temperatures (*Bakhshandeh et al., 2017*; *Rowse and Finch-Savage, 2010*), suggesting that HT
253   estimates were not consistent across variable temperatures. In other words, grouping of

254 normalized observations resulted in large shifts in the theoretical threshold or base water
255 potential ($\Psi_b(g)$) that can prevent the fraction of germination as temperature increases (*Rong et*
256 *al., 2015*). Furthermore, when the distribution of $\Psi_b(g)$ overlaps with 0 MPa at a given
257 temperature, germination of some seeds may be inhibited (Alvarado and Bradford, 2002; Larsen
258 et al., 2004; Watt et al., 2011). For this reason, Alvarado and Bradford (2002) developed the
259 HTT model to account for the linear increase of $\Psi_b(g)$ value as temperature increased above T_o in
260 order to eliminate the positive shift in $\Psi_b(g)$ values at supra-optimal temperatures. This modified
261 model can quantify and predict both final germination percentage and germination rate across
262 different temperatures and water potential levels at which seed germination occurs (*Bakhshandeh*
263 *et al., 2015*; *Rowse and Finch-Savage, 2010*) as we observed for germination time course of *A.*
264 *tenuissimum* seeds at supra-optimal temperatures, which were well described by HTT model
265 (i.e., $R^2 = 0.81$).

266 **Model parameters and their biological roles**
267 Because changes in dormancy state are related to Ψ_b (*Meyer et al., 2000*) and high temperatures
268 often induce secondary dormancy, soil water availability is critical for seed germination at supra-
269 optimal temperatures (*Hills et al., 2003*). Likewise, values of $\Psi_b(50)$ (-0.74 to -0.16 MPa)
270 determined in our analysis revealed that seeds of *A. tenuissimum* are relatively sensitive to water
271 restrictions at temperatures above T_o. Thus, seeds of *A. tenuissimum* should be germinated at
272 sub-optimal temperatures to enhance crop establishment in arid and semi-arid regions. Results
273 from HT analysis also indicated that the minimum value of $\Psi_b(50)$ was observed at 11 °C and
274 then increased, particularly in supra-optimal temperature ranges. Similar to our results, the linear
275 increase of $\Psi_b(50)$ has been observed in zucchini (*Atashi et al., 2015*), watermelon (Bakhshandeh
276 et al., 2015), and sesame (*Bakhshandeh et al., 2017*). In general, the $\Psi_b(50)$ value of a seed lot
277 gives an indication of its tolerance to water stress. If water potential levels are more negative
278 than $\Psi_b(50)$, germination times will be extended and germination rates will be reduced
279 (*Bradford, 2002*). This could be caused by a decrease in both enzyme activity and oxygen
280 availability during the seed germination period, particularly when germinated at supra-optimal
281 temperatures (*Bewley et al., 2013*). When soil temperature approaches T_o, less negative water
282 potential levels will cause an increase in the activity of enzymes and water uptake rate (*Kebreab*
283 *and Murdoch, 1999*).
284   Base water potential coefficient (σ_{Ψ_b}) is related to life history strategy of various species
285 (*Bradford, 1990*) and indicates the uniformity of seed germination among individual seeds
286 within a seed lot. A smaller value of σ_{Ψ_b} represents an increasingly uniform germination among
287 seed population (*Bradford and Still, 2004*; *Bidgolya et al., 2018*). The values of σ_{Ψ_b} we estimated
288 for *A. tenuissimum* seeds varied from 0.20 to 0.37 MPa, indicating that there was less variation in
289 Ψ_b among individual seeds and that uniform germination was observed. This pattern is likely a
290 reflection of survival adaptations to harsh environments. Under initial favorable soil temperature
291 and water availability, faster and uniform germination will allow plants to possibly dominate a
292 plant community in space and time (*Wang et al., 2009*). In contrast, most plant populations must
293 adopt a different germination strategy to mitigate the harsh environment-induced damage on

294   germination by allowing a few seeds to rapidly germinate, and then delaying germination until
295   consistent suitable environment conditions are reached before the remaining seeds germinate
296   (*Bradford, 1990*; *Batlla et al., 2009*; *Watt et al., 2011*; *Rong et al., 2015*). Consistent with our
297   results, the variation of Ψ_b was small and σ_{Ψ_b} varied from 0.16 to 0.31 MPa among *Vicia sativa*
298   seeds (*Liu, 2010*), indicating that the long-term cultivation and domestication can result in
299   uniform germination.
300   The hydrotime (MPa d) constant of the seeds required for germination (θ_H) represents the
301   inherent speed of seed germination in a seed lot (*Bradford and Still, 2004*). Our results showed
302   that θ_H declined from 6.4 to 3.0 MPa d as temperature increased from 11 °C to 24 °C, indicating
303   that germination rate was faster at higher temperatures (Fig. 2, Table 1). Similarly, other studies
304   reported that θ_H was constant in supra-optimal temperature ranges, but it increased as
305   temperature declined in the range of sub-optimal temperatures (*Bakhshandeh et al., 2015*; *Dahal*
306   *and Bradford, 1994*). Thus, seed germination was greatly altered with decreasing temperature.
307   Seed germination responses to temperature are commonly characterized with three cardinal
308   temperatures (T_b, T_o and T_c) estimated according to the HTT model (*Bewley et al., 2013*). These
309   cardinal temperatures of *A. tenuissimum* seeds were $T_b = 7.0$ °C, $T_o = 20.5$ °C, and $T_c(50) = 27.2$
310   °C, respectively. In practical terms, these values suggest *A. tenuissimum* seeds should not be
311   sown in soils where temperature do not exceed 7.0 °C. Maximum final germination percentage
312   would be observed as soil temperature approaches 20.5 °C, a value when some seeds within the
313   population will probably germinate quickly if they are not exposed to water stress or dormancy
314   induction within optimal ranges (*Rong et al., 2015*; *Windauer et al., 2012*). In addition, because
315   seeds of *A. tenuissimum* germinated in a relatively narrow range of temperature according to
316   estimations of $T_c(50)$, seeds of *A. tenuissimum* are likely unable to tolerate high soil temperature.
317   From a crop production standpoint, our results document that seed germination of *A.*
318   *tenuissimum* occurs over a soil temperature range of 7.0 to 27.2 °C, but 20.5 °C is the optimal
319   temperature. These estimated cardinal temperatures are consistent with wild *Allium* species
320   (*Zhao et al., 2011*).

Conclusions

322   The mathematical models or the estimated value of parameters can be used to quantitatively
323   predict the seed germination of *A. tenuissimum* under various T and Ψ conditions. Soil
324   temperature for seed germination of *A. tenuissimum* should be at the range of 7.0 °C to 27.2 °C,
325   and the optimum temperature is 20.5 °C. The water potential should be less negative than -0.67
326   MPa. The relatively lower T_b and more negative $\Psi_b(50)$ indicate that this wild *Allium* species
327   might be established in arid and semi-arid regions, while relatively narrow threshold in response
328   to T and Ψ variations might sufficiently delay or even prevent seed germination in extreme arid
329   or harsh desert regions.

Acknowledgments

331   This research was supported by the National Key Research and Development Program of China
332   (2016YFC0500603), the National Natural Science Foundation of China (31772653) and National

333 Natural Science Foundation of China (31472136).

References

335 Abdellaoui R, Boughalleb F, Zayoud D, Neffati M, Bakhshandeh E (2019) Quantification of
336   *Retama raetam* seed germination response to temperature and water potential using
337   hydrothermal time concept. Environ Exp Bot 157:211-216 DOI
338   10.1016/j.envexpbot.2018.10.014.

339 Alvarado V, Bradford KJ (2002) A hydrothermal time model explains the cardinal temperatures
340   for seed germination. Plant Cell Environ 25:1061-1069 DOI 10.1046/j.1365-
341   3040.2002.00894.x.

342 Atashi S, Bakhshandeh E, Mehdipour M, Jamali M, Teixeira Da Silva JA (2015) Application of
343   a hydrothermal time seed germination model using the Weibull distribution to describe base
344   water potential in zucchini (*Cucurbita pepo* L.). J Plant Growth Regul 34:150-157 DOI
345   10.1007/s00344-014-9452-y.

346 Bakhshandeh E, Atashi S, Hafeznia M, Pirdashti H (2013) Quantification of the response of
347   germination rate to temperature in sesame (*Sesamum indicum*). Seed Sci Technol 41:469-473
348   DOI 10.15258/sst.2013.41.3.14.

349 Bakhshandeh E, Atashi S, Hafeznia M, Pirdashti H, Teixeira Da Silva JA (2015) Hydrothermal
350   time analysis of watermelon (*Citrullus vulgaris* cv. 'Crimson sweet') seed germination. Acta
351   Physiol Plant 37:1738 DOI 10.1007/s11738-014-1738-y.

352 Bakhshandeh E, Gholamhossieni M (2018) Quantification of soybean seed germination response
353   to seed deterioration under PEG-induced water stress using hydrotime concept. Acta Physiol
354   Plant 40:126 DOI 10.1007/s11738-018-2700-1

355 Bakhshandeh E, Gholamhossieni M (2019) Modelling the Effects of Water Stress and
356   Temperature on Seed Germination of Radish and Cantaloupe. J Plant Growth Regul 38:1402-
357   1411 DOI 10.1007/s00344-019-09942-9

358 Bakhshandeh E, Jamali M, Afshoon E, Gholamhossieni M (2017) Using hydrothermal time
359   concept to describe sesame (*Sesamum indicum* L.) seed germination response to temperature
360   and water potential. Acta Physiol Plant 39:250 DOI 10.1007/s11738-017-2549-8.

361 Batlla D, Grundy A, Dent KC, Clay HA, Finch-Savage WE (2009) A quantitative analysis of
362   temperature-dependent dormancy changes in *Polygonum aviculare* seeds. Weed Res 49:428-
363   438 DOI 10.1111/j.1365-3180.2009.00706.x.

364 Belo RG, Tognetti J, Benech-Arnold R, Izquierdo NG (2014) Germination responses to
365   temperature and water potential as affected by seed oil composition in sunflower. Ind Crop
366   Prod 62:537-544 DOI 10.1016/j.indcrop.2014.09.029.

367 Bewley JD, Black M (1994) Seeds: physiology of development and germination. New
368   York:Plenum Press

369 Bewley JD, Bradford K, Hilhorst H, Nonogaki H (2013) Seeds: physiology of development,
370   germination and dormancy. 3rd edn. Springer, New York, pp 407

371 Bidgolya RO, Balouchi H, Soltani E, Moradi A (2018) Effect of temperature and water potential
372   on *Carthamus tinctorius* L. seed germination: Quantification of the cardinal temperatures and

373   modeling using hydrothermal time. Ind Crop Prod 113:121-127 DOI
374   10.1016/j.indcrop.2018.01.017.
375 Bradford KJ (1990) A water relations analysis of seed germination rates. Plant Physiol 94:840-
376   849 DOI 10.1104/pp.94.2.840.
377 Bradford KJ (2002) Applications of hydrothermal time to quantifying and modeling seed
378   germination and dormancy. Weed Sci 50:248-260 DOI 10.1614/0043-1745.
379 Bradford KJ, Still DW (2004) Applications of hydrotime analysis in seed testing. Seed Technol
380   26:75-85 https://www.jstor.org/stable/23433495.
381 Dahal P, Bradford KJ (1990) Effects of priming and endosperm integrity on seed-germination
382   rates of tomato genotypes. 2. Germination at reduced water potential. J Exp Bot 41:1441-
383   1453 DOI 10.1093/jxb/41.11.1441.
384 Dahal P, Bradford KJ (1994) Hydrothermal time analysis of tomato seed germination at
385   suboptimal temperature and reduced water potential. Seed Sci Res 4:71-80 DOI
386   10.1017/S096025850000204X.
387 Fakhfakh LM, Anjum NA, Chaieb M (2018) Effects of temperature and water limitation on the
388   germination of *Stipagrostis ciliata* seeds collected from Sidi Bouzid Governorate in Central
389   Tunisia. J Arid Land 10:304-315 DOI 10.1007/s40333-018-0050-x.
390 Fischer RA, Turner NC (1978) Plant productivity in the arid and semiarid zones. Annu Rev Plant
391   Physiol 29:277-317 DOI 10.1146/annurev.pp.29.060178.001425.
392 Gummerson RJ (1986) The effect of constant temperatures and osmotic potentials on the
393   germination of sugar beet. J Exp Bot 37:729-741 DOI 10.1093/jxb/37.6.729.
394 He XL (2008) Study on biology characteristics and exploitation and utilization of *Allium*
395   *tenuissimum* L. J Anhui Agr Sci 36:1814 [In Chinese]
396 Herranz JM, Ferrandis P, Martínez-Sánchez JJ (1998) Influence of heat on seed germination of
397   seven mediterranean leguminosae species. Plant Ecol 136(1):95-103 DOI
398   10.1023/A:1009702318641.
399 Hills PN, Staden JV, Thomas TH (2003) Thermoinhibition of seed germination. S Afr J Bot
400   69:455-461 DOI 10.1016/S0254-6299(15)30281-7.
401 Horn KJ, Nettles R, Clair SBS (2015) Germination response to temperature and moisture to
402   predict distributions of the invasive grass red brome and wildfire. Biol Invasions 17:1849-
403   1857 DOI 10.1007/s10530-015-0841-3.
404 Izquierdo J, Bastida F, Lezaún JM, Sánchez Del Arco MJ, Gonzalez-Andujar JL (2013)
405   Development and evaluation of a model for predicting *Lolium rigidum* emergence in winter
406   cereal crops in the Mediterranean area. Weed Res 53:269-278 DOI 10.1111/wre.12023.
407 Juan-Vicedo J, Fernández-Pereira J, Ríos S, Casas, JL, Martín I (2016) Seed germination and
408   storage behaviour of lapiedra martinezii (amaryllidaceae). Seed Sci and Technol 44(1):199-
409   206 DOI 10.15258/sst.2016.44.1.02
410 Kebreab E, Murdoch AJ (1999) Modelling the effects of water stress and temperature on
411   germination rate of *Orobanche aegyptiaca* seeds. J Exp Bot 50:655-664 DOI
412   10.1093/jxb/50.334.655.

Larsen SU, Bailly C, Come D, Corbineau F (2004) Use of the hydrothermal time model to analyse interacting effects of water and temperature on germination of three grass species. Seed Sci Res 14:35-50 DOI 10.1079/SSR2003153.

Li LY, Zhang WF (2011) Study on the condiment industrialization of *Allium tenuissimum* L. Heilongjiang Agr Sci (9):104-106 [In Chinese].

Li LY, Zhang WF, Zhang SZ, Zheng LS, Fan LS (2011) Study on biology characteristics of developmental rhythm of annual plants of *Allium tenuissimum* L. Heilongjiang Agr Sci (5):68-70 [In Chinese]

Li LY, Zhang WF, Zheng LS, Guo YD, Li QZ (2013) Artificial cultivation techniques of *Allium tenuissimum* L. Heilongjiang Agr Sci (12):161-162 [In Chinese].

Liu GX, Wang BB, Lin YJ, Liang X, An Y, Liu ZK (2016) Analysis of agronomic characters of four *Allium* species under wild and cultivated conditions. North Hortic (4):1-5 [In Chinese].

Liu SS (2010) A study on germination threshold models of common vetch (*Vicia sativa* L.) seeds. Dissertation, China Agricultural University [In Chinese].

Marques I, Draper D (2012) Seed germination and longevity of autumn-flowering and autumn-seed producing Mediterranean geophytes. Seed Sci Res 22(4):299-309 DOI 10.1017/S0960258512000153

Mccartan SA, Jinks RL, Barsoum N (2015) Using thermal time models to predict the impact of assisted migration on the synchronization of germination and shoot emergence of oak (*quercus robur* L.). Ann of Forest Sci 72(4):479-487 DOI 10.1007/s13595-014-0454-5

Meyer SE, Debaenegill SB, Allen PS (2000) Using hydrothermal time concepts to model seed germination response to temperature, dormancy loss, and priming effects in *Elymus elymoides*. Seed Sci Res 10:213-223 DOI 10.1017/S0960258500000246.

Rawlins JK, Roundy BA, Davis SM, Egget D (2012) Predicting germination in semi-arid wildland seedbeds. I. Thermal germination models. Environ Exp Bot 76:60-67 DOI 10.1016/j.envexpbot.2011.10.003.

Rong Y, Li H, Johnson DA (2015) Germination response of *Apocynum venetum* seeds to temperature and water potential. J Appl Bot Food Qual 88:202-208 DOI 10.5073/JABFQ.2015.088.029.

Ronnenberg K, Wesche K, Hensen I (2008) Germination ecology of Central Asian *Stipa* spp: differences among species, seed provenances, and the importance of field studies. Plant Ecol 196:269-280 DOI 10.1007/s11258-007-9351-4.

Rowse HR, Finch-Savage WE (2010) Hydrothermal threshold models can describe the germination response of carrot (*Daucus carota*) and onion (*Allium cepa*) seed populations across both sub- and supra-optimal temperatures. New Phytol 158:101-108 DOI 10.1046/j.1469-8137.2003.00707.x.

Saleem MH, Ali S, Seleiman MF, Rizwan M, Rehman M, Aisha Akram N, Liu L, Alotaibi M, Al-Ashkar I, Mubushar M (2019) Assessing the Correlations between Different Traits in Copper-Sensitive and Copper-Resistant Varieties of Jute (*Corchorus capsularis* L.). Plants 8: 545 DOI 10.3390/plants8120545

453   Schütz W, Rave G (1999) The effect of cold stratification and light on the seed germination of
454   temperate sedges (*Carex*) from various habitats and implications for regenerative strategies.
455   Plant Ecol 144:215-230 DOI 10.1023/A:1009892004730.
456   Soltani E, Adeli R, Akbari GA, Ramshini H (2017) Application of hydrotime model to predict
457   early vigour of rapeseed (*Brassica napus* L.) under abiotic stresses. Acta Physiol Plant
458   39:252 DOI 10.1007/s11738-017-2552-0.
459   Song B, Niu S, Wan S (2016) Precipitation regulates plant gas exchange and its long-term
460   response to climate change in a temperate grassland. J Plant Ecol 9:531-541 DOI
461   10.1093/jpe/rtw010.
462   Tobe K, Zhang L, Qiu GY, Shimizu H, Omasa K (2001) Characteristics of seed germination in
463   five non-halophytic Chinese desert shrub species. J Arid Environ 47:191-201 DOI
464   10.1006/jare.2000.0689.
465   Torabi B, Soltani E, Archontoulis SV, Rabii A (2016) Temperature and water potential effects
466   on *Carthamus tinctorius* L. seed germination: measurements and modeling using
467   hydrothermal and multiplicative approaches. Braz J Bot 39:427-436 DOI 10.1007/s40415-
468   015-0243-x.
469   Trudgill DL, Honek A, Li D, Van Straalen, NM (2005) Thermal time-concepts and utility. Ann
470   Appl Biol 146:1-14 DOI 10.1111/j.1744-7348.2005.04088.x.
471   Wang JH, Du GZ, Cui XL, Zheng XF, Qi W (2009) Germination characteristics of 61 common
472   woody species from the eastern Qinghai-Tibet Plateau of China and their life history
473   correlates. Chinese J Plant Ecol 33:171-179 [In Chinese].
474   Watt MS, Bloomberg M, Finch-Savage WE (2011) Development of a hydrothermal time model
475   that accurately characterises how thermoinhibition regulates seed germination. Plant Cell
476   Environ 34:870-876 DOI 10.1111/j.1365-3040.2011.02292.x.
477   Watt MS and Bloomberg M (2012) Key features of the seed germination response to high
478   temperatures. New Phytol, 196:332-336 DOI 10.1111/j.1469-8137.2012.04280.x.
479   Windauer LB, Martinez J, Rapoport D, Wassner D, Benech-Arnold R (2012) Germination
480   responses to temperature and water potential in *Jatropha curcas* seeds: a hydrotime model
481   explains the difference between dormancy expression and dormancy induction at different
482   incubation temperatures. Ann Bot 109:265-273 DOI 10.1093/aob/mcr242.
483   Xu MJ, Zhang J, Li MP, Yu LG, Guo CX, Zhang SW (2017) Analysis of the volatile compounds
484   in the flowers of *Allium tenuissimum* by headspace-gas chromatography-olfactometry-mass
485   spectrometry. Food Sci 38:199-203 [In Chinese].
486   Zhang WF, Li LY, Zheng LS (2014) Harvesting and preservation techniques of *Allium
487   tenuissimum* L. Modern Agr Sci Technol (17):124-125 [In Chinese].
488   Zhang XL, Liu LM (2012) Study on extraction process of flower essential oil in *Allium
489   tenuissimum* L. by supercritical CO_2 fluid. China Condiment 37:74-78 [In Chinese].
490   Zhao JH (2010) A study on ecological adaptability and reproduction feature of three wild *Allium*
491   plants. Dissertation, Inner Mongolia Agricultural University [In Chinese].
492   Zhao JH, Li QF, Badema GLB (2011) Studies on seed imbibition characteristics of three wild

493   *Allium* plants in Inner Mongolia. Seed 30:95-98 [In Chinese].

Parameters of the hydrotime model characterizing germination of *A. tenuissimum* seeds across a range of temperatures.

The hydrotime time model (Eq. 2) was fitted to data from four water potential levels (0, -0.2, -0.4 and -0.6 MPa) at five temperature regimes (11, 15, 20, 24 and 28 °C). θ_H, hydrotime constant; $\Psi_b(50)$, base water potential for 50% seed germination; $\sigma_{\psi b}$, standard deviation for $\Psi_b(g)$; R^2, coefficient of determination

Temperature (°C)	θ_H (MPa d)	$\Psi_b(50)$ (MPa)	$\sigma_{\Psi b}$ (MPa)	R^2
11	6.4	-0.74	0.20	0.95
15	4.4	-0.60	0.29	0.97
20	4.2	-0.49	0.27	0.92
24	3.0	-0.40	0.28	0.90
28	3.0	-0.16	0.37	0.94

Parameters of the hydrothermal time model characterizing germination of *A. tenuissimum* seeds at sub-optimal and supra-optimal *T*.

T_b, base temperature; T_o, optimal temperature; θ_{HT}, hydrothermal time constant; $\Psi_b(50)$, base water potential for 50% seed germination; $\sigma_{\psi b}$, standard deviation for $\Psi_b(g)$; R^2, coefficient of determination; K_T, the slope of the relationship between $\Psi_b(50)$ and temperatures when *T* exceeds T_o. $T_c(50)$, ceiling temperature to germination of 50%. The value of $T_c(50)$ was calculated by parameters found after fitting the HTT model at supra-optimal *T* (Eq. 6).

hydrothermal time model Parameters	sub-optimal T	supra-optimal T
T_b (°C)	7.0	7.0
θ_{HT} (MPa °C d)	43.9	43.9
$\Psi_b(50)$ (MPa)	-0.67	-0.67
$\sigma_{\Psi b}$ (MPa)	0.28	0.32
R^2	0.89	0.81
T_o (°C)	-	20.5
$T_c(50)$ (°C)	-	27.2
K_T (MPa °C^{-1})	-	0.1

Figure 1

Mean (± standard error) final germination percentage of *A. tenuissimum* seeds under variable temperature (*T* = 11, 15, 20, 24, and 28 °C) and water potential (*Ψ* = 0, -0.2, -0.4, and -0.6 MPa) levels
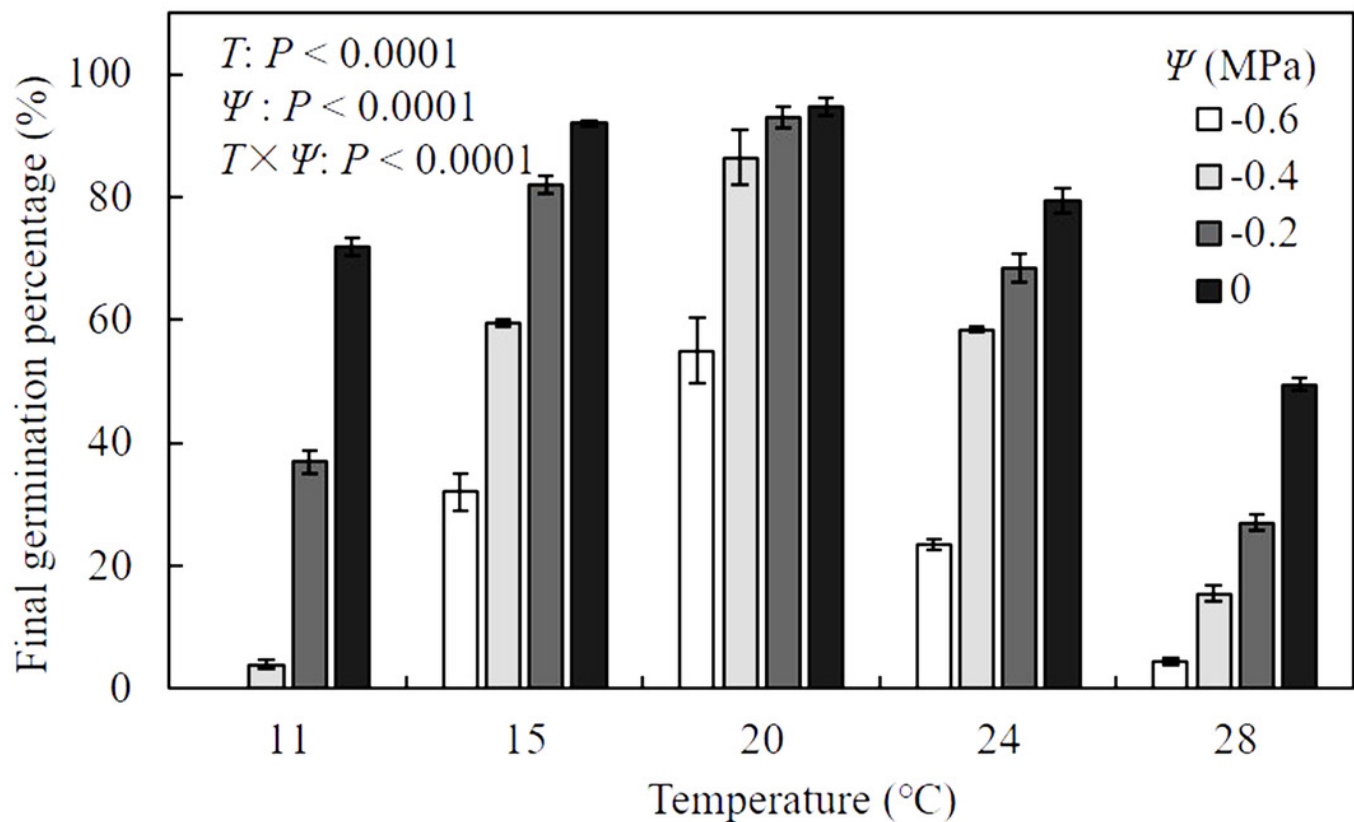
Figure 2

Germination time courses of *A. tenuissimum* seeds across a range of water potential and temperature (A-E) and normal distributions of the relative frequencies of base water potential at each temperature (11, 15, 20, 24 and 28 °C) (F-G).

Symbols represent actual data and lines indicate values predicted by probit analysis using the parameters presented in Table 1
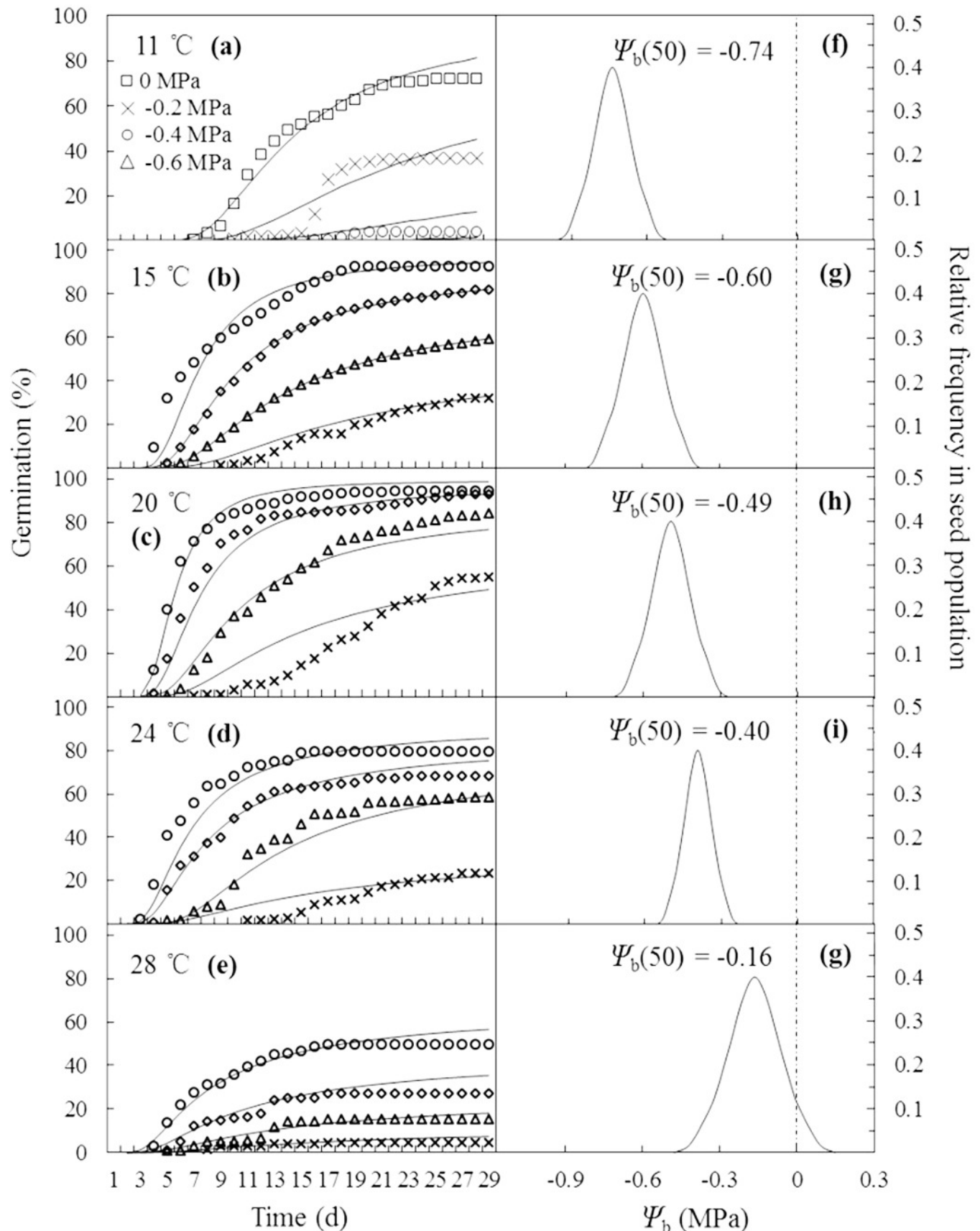
Figure 3

Normalized time courses of the sub- and supra-optimal hydrotime models.

(A) Germination data from Fig. 2A–C is plotted on a normalized thermal time scale showing the predicted time courses in water according to the parameters of sub-optimal T shown in Table 2. (B) Germination data from Fig. 2D-E are plotted on a normalized time scale showing the predicted time courses in water according to the parameters of supra-optimal T shown in Table 2. (C) Germination time courses across all T and Ψ shown in Fig. 2A-E merged into a single normalized thermal time scale